q-breathers in Fermi-Pasta-Ulam chains: Existence, localization, and stability

S. Flach,[1] M. V. Ivanchenko,[2] and O. I. Kanakov[2]
[1]*Max-Planck-Institut für Physik Komplexer Systeme, Nöthnitzer Strasse 38, D-01187 Dresden, Germany*
[2]*Department of Radiophysics, Nizhny Novgorod University, Gagarin Avenue, 23, 603950 Nizhny Novgorod, Russia*
(Received 30 August 2005; published 24 March 2006)

The Fermi-Pasta-Ulam (FPU) problem consists of the nonequipartition of energy among normal modes of a weakly anharmonic atomic chain model. In the harmonic limit, each normal mode corresponds to a periodic orbit in phase space and is characterized by its wave number q. We continue normal modes from the harmonic limit into the FPU parameter regime and obtain persistence of these periodic orbits, termed here q-breathers (QB). They are characterized by time periodicity, exponential localization in the q-space of normal modes, and linear stability up to a size-dependent threshold amplitude. Trajectories computed in the original FPU setting are perturbations around these exact QB solutions. The QB concept is applicable to other nonlinear lattices as well.

DOI: 10.1103/PhysRevE.73.036618 PACS number(s): 05.45.−a, 63.20.Pw, 63.20.Ry

I. INTRODUCTION

In 1955, Fermi, Pasta, and Ulam (FPU) published their celebrated report on thermalization of arrays of particles connected by weakly nonlinear springs [1]. Instead of the expected equipartition of energy among the normal modes of the systems, FPU observed that energy, initially placed in a low-frequency normal mode of the linear problem with a frequency ω_q and a corresponding wave number q, stayed almost completely locked within a few neighbor modes, instead of being distributed among all modes of the system. Moreover, recurrence of energy to the originally excited mode was observed. The door was thus opened to study the fundamental physical and mathematical problem of energy equipartition and ergodicity in nonlinear systems, which involves the Kolmogorov-Arnold-Moser (KAM) theorem, thresholds between regular and chaotic dynamics, and soliton-bearing integrable models.

From the present perspective, the FPU observation (equally coined FPU problem or FPU paradox) appears to consist of three major ingredients: (FPU-1) for suitable parameter ranges (energy, system size, nonlinearity strength), low-frequency excitations are localized in q-space of the normal modes; (FPU-2) recurrence of energy to an initially excited low-frequency mode is observed; (FPU-3) different thresholds upon tuning the parameters are observed—a weak stochasticity threshold (WST) which separates regular and chaotic dynamics, yet possibly preserving the localization character in q-space, and an equipartition threshold (ET), also coined strong stochasticity threshold, separating localized from delocalized dynamics in q-space (see Refs. [2–4] for a review).

Two major approaches were developed. The first one, taken by Zabusky and Kruskal, was to analyze the dynamics of the nonlinear chain in the continuum limit, which led to a pioneering observation of solitary waves [5]. It took (FPU-1) as given, and aimed at obtaining quantitative estimates for (FPU-2). A second approach was proposed by Izrailev and Chirikov [6], who associated energy equipartition with dynamical chaos and aimed at an analytical estimate of the ET by computing the overlap of nonlinear resonances [7], which leads to strong dynamical chaos ensuring energy equipartition. Below the threshold, the dynamics is regular and, thus, no equipartition should occur. It aimed mainly at (FPU-3). Several other analytical [8,9] and numerical [10–12] threshold estimates have been published since, and will be discussed below. Note that similar effects have been observed in many other nonlinear discrete chain or field equations on a finite spatial domain; see, e.g., Ref. [13].

In this work, we show that stable periodic orbits, which are coined q-breathers (QB), persist in the nonlinear FPU chain and are exponentially localized in q-space of normal modes. The existence of these orbits was first reported in Ref. [14]. Stability of these periodic orbits implies that small perturbations initially localized on a q-breather will stay localized in q-space as well. Thus these perturbations will evolve in a nearly regular fashion for long times effectively exciting only a small number of degrees of freedom. Recurrence times—to come close to an initial point again—will be much shorter than the general Poincaré recurrence times estimate, which are derived from exciting all available degrees of freedom [15]. Upon increasing the nonlinearity of the system, QBs will turn from stable to unstable at certain threshold values, allowing for low-dimensional chaotic evolution of nearby trajectories on long time scales. The localization length in q-space depends on these parameters as well, and at critical parameter values QBs delocalize, possibly leading to equipartition. The q-breather concept allows us thus to address simultaneously all three FPU ingredients. At the same time, it can be extended to completely different lattice systems and even to nonlinear field equations.

In the present work, we construct QBs continuing them from the linear case and study their properties both numerically and by an analytical asymptotic calculation. We compare the thresholds of QB localization and stability to the various stochasticity thresholds mentioned above. Finally, we show the persistence of QBs in thermal equilibrium and during long transient processes.

II. THE MODEL

The FPU system is a chain of N equal masses coupled by nonlinear springs with the equations of motion containing quadratic (the α-model)

$$\ddot{x}_n = (x_{n+1} - 2x_n + x_{n-1}) + \alpha[(x_{n+1} - x_n)^2 - (x_n - x_{n-1})^2] \tag{1}$$

or cubic (the β-model)

$$\ddot{x}_n = (x_{n+1} - 2x_n + x_{n-1}) + \beta[(x_{n+1} - x_n)^3 - (x_n - x_{n-1})^3] \tag{2}$$

interaction terms, where x_n is the displacement of the nth particle from its original position, and fixed boundary conditions are taken $x_0 = x_{N+1} = 0$. A canonical transformation

$$x_n(t) = \sqrt{\frac{2}{N+1}} \sum_{q=1}^{N} Q_q(t) \sin\left(\frac{\pi q n}{N+1}\right) \tag{3}$$

takes into the reciprocal wave-number space with N normal mode coordinates $Q_q(t)$. The equations of motion then read

$$\ddot{Q}_q + \omega_q^2 Q_q = -\frac{\alpha}{\sqrt{2(N+1)}} \sum_{l,m=1}^{N} \omega_q \omega_l \omega_m B_{q,l,m} Q_l Q_m \tag{4}$$

for the FPU-α chain (1) and

$$\ddot{Q}_q + \omega_q^2 Q_q = -\frac{\beta}{2(N+1)} \sum_{l,m,n=1}^{N} \omega_q \omega_l \omega_m \omega_n C_{q,l,m,n} Q_l Q_m Q_n \tag{5}$$

for the FPU-β chain (2). Here the coupling coefficients $B_{q,l,m}$ and $C_{q,l,m,n}$ are given by

$$B_{q,l,m} = \sum_{\pm} (\delta_{q \pm l \pm m,0} - \delta_{q \pm l \pm m,2(N+1)}), \tag{6}$$

$$C_{q,l,m,n} = \sum_{\pm} (\delta_{q \pm l \pm m \pm n,0} - \delta_{q \pm l \pm m \pm n,2(N+1)} - \delta_{q \pm l \pm m \pm n,-2(N+1)}). \tag{7}$$

The sum in Eqs. (6) and (7) is taken over all four or eight combinations of signs, respectively. The normal mode frequencies

$$\omega_q = 2 \sin \frac{\pi q}{2(N+1)} \tag{8}$$

are nondegenerate.

III. A CROSSLINK TO DISCRETE BREATHERS

The system of equations (4) and (5) corresponds to a network of oscillators with different eigenfrequencies. These oscillators are interacting with each other via *nonlinear* interaction terms, yet being long-ranged in q-space. Let us discuss the relation of this problem to the well-known field of discrete breathers [16–18].

Neglecting the nonlinear terms in the equations of motion, the q-oscillators get decoupled, each conserving its energy

$$E_q = \frac{1}{2}(\dot{Q}_q^2 + \omega_q^2 Q_q^2) \tag{9}$$

in time. Especially, we may consider the excitation of only one of the q-oscillators, i.e., $E_q \neq 0$ for $q \equiv q_0$ only. Such excitations are trivial time-periodic and q-localized solutions (QBs) for $\alpha = \beta = 0$.

This setting is similar to the case of discrete breathers (DB), which are time-periodic and spatially localized excitations, e.g., on networks of interacting *identical anharmonic* oscillators, which survive continuation from the trivial limit of zero coupling [19]. Notably, DBs exist also in FPU lattices [18] and existence proofs has been obtained as well [20–22]. The reason for the generic existence of DBs is twofold: the nonlinearity of each oscillator allows us to tune its excitation frequency out of resonance with other nonexcited oscillators. The case of a *linear* coupling on the lattice ensures a bound spectrum of small-amplitude plane waves, and thus allows for the escape of resonances of a DB frequency and its higher harmonics with that spectrum. The spatial localization of DBs in such a case is typically exponential for short-range interactions [16]. Among the wealth of theoretical results, we stress two here. First, if the coupling on the lattice is short-ranged but purely *nonlinear*, the DB localizes in space *superexponentially* [23]. Second, if the coupling is algebraically decaying on the lattice, DBs localize only algebraically as well [24].

Let us compare these findings to the q-breather setting. For zero nonlinearity the *nonidentical* q-oscillators (9) are harmonic. For all cases, the following nonresonance condition holds [25]:

$$\omega_q \neq n\omega_{q_0}, \tag{10}$$

where $q_0 \neq q$ and n is any integer. That allows continuation of a trivial QB orbit from zero nonlinearity into the domain of nonzero nonlinearity, similar to the existence proof of discrete breathers by MacKay and Aubry [19] by continuation from the uncoupled limit of anharmonic oscillators. Their proof, however, cannot be applied directly to the case considered here, because it requires the period of each oscillator to depend on its energy.

But in fact that is not needed, since the mere persistence of N periodic orbits under the nonresonance condition (10) in a class of Hamiltonian systems, which includes the system considered, was proved by Lyapunov in 1892 [26] (especially Chap. II, Sec. 45 starting on p. 174). Note that this proof operates at fixed nonzero nonlinearity, in some phase space neighborhood of the stable equilibrium. We sketch the main ingredients that allow us to construct a proof of persistence of periodic orbits by tuning the nonlinearity in Appendix A. That scheme can be used as well in computational procedures. For that, one considers the map of all mode coordinates and velocities with $q \neq q_0$ onto themselves. The map condition is to start with $Q_{q_0}(t=0) = A > 0$, $\dot{Q}_{q_0}(t=0) = 0$ and to measure the mode coordinates and velocities for $q \neq q_0$ after the time $\tau > 0$ when $\dot{Q}_{q_0}(\tau) = 0$ and $Q_{q_0}(\tau) > 0$. A fixed point of that map corresponds to a periodic orbit.

As for their degree of localization in q-space (if any), the above results on DBs suggest that two mechanisms counteract: purely nonlinear interaction favors stronger than exponential localization, while long-range interaction tends to delocalize the QB. We also recall that the seemingly simple problem of periodic motion of a classical particle in an anharmonic potential of the FPU type follows from the differential equation

$$\ddot{x} = -x - \alpha x^2 - \beta x^3. \tag{11}$$

Bounded motion at some energy E yields a solution that is periodic with some period $T(E)=2\pi/\Omega$ and can be represented by a Fourier series

$$x(t) = \sum_k A_k e^{ik\Omega t}, \tag{12}$$

which leads to algebraic equations for the Fourier coefficients A_k,

$$A_k = k^2\Omega^2 A_k - \alpha \sum_{k_1} A_{k_1} A_{k-k_1} - \beta \sum_{k_1,k_2} A_{k_1} A_{k_2} A_{k-k_1-k_2}. \tag{13}$$

Note that Eq. (13) have similar properties as compared to Eqs. (4) and (5)—interaction between the Fourier coefficients is nonlinear but long-ranged. Yet it is well known that the bounded solutions (12) to Eq. (11) are analytic functions $x(t)$ and thus the Fourier series coefficients A_k converge exponentially fast with k [27].

Let us summarize this section by stating that from a mathematical point of view, q-breather existence and their properties can be treated in a similar way to the methodology of discrete breather theory. The two different types of excitations, localized in real space and localized in reciprocal q-space, have much in common when represented in their natural phase space basis choice. Both representations are connected to each other by a simple canonical transformation, which is nothing but a rotation of the phase space basis. In the following, we will use analytical and computational tools developed for discrete breathers and analyze the properties of q-breathers.

IV. q-BREATHERS IN THE α-FPU SYSTEM

A. Numerical results

Let us consider the α-model and start with showing the evolution of the original FPU trajectory for $\alpha=0.25$, $N=32$, and an energy $E=0.077$ placed initially into the mode with $q_0=1$. We plot the time dependence of the mode energies $E_q(t)$ in Fig. 1 for the first five modes. The period of the slowest ($q_0=1$) harmonic mode is $T_1=2\pi/\omega_1\approx 66.02$. We nicely observe slow processes of redistribution of mode energies, recurrences, and also even slower modulations of recurrence amplitudes on time scales of the order of 10^5. Note also that on time scales comparable to T_1, all mode energies show small additional oscillations, and it is easy to see that they correspond to frequencies that are multiples of ω_1. The localization in q-space is also nicely observed, with the maximum of E_5 being eight times smaller than that of E_1.

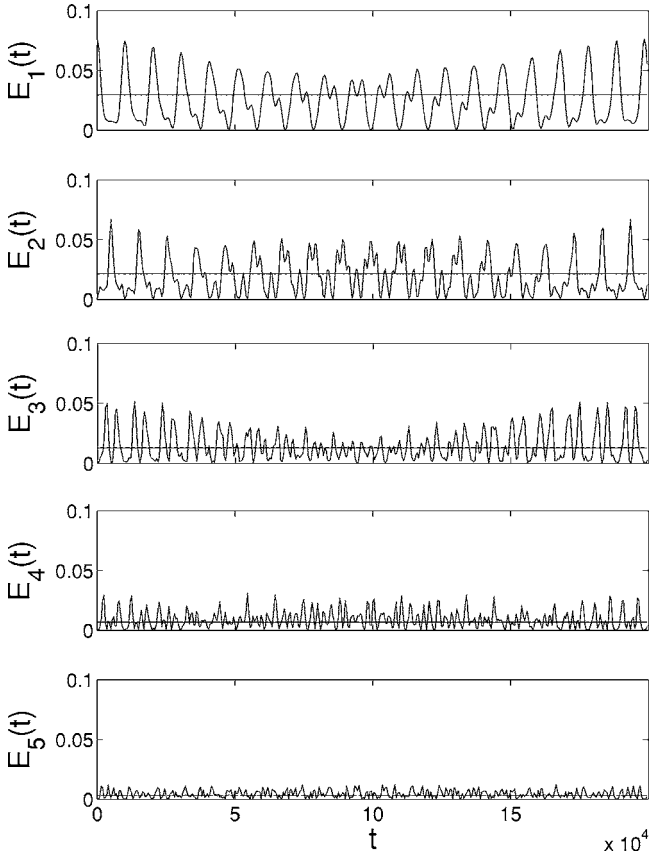

FIG. 1. Evolution of the linear mode energies for the first five modes on a large time scale for (i) the original FPU trajectory for $\alpha=0.25$, $E=0.077$, $N=32$ [1] (oscillating curves) and (ii) the exact QB solution (almost straight lines).

In order to construct a q-breather, let us choose first $\alpha=0$, excite a normal mode with $q=q_0$ to the energy $E_{q_0}=E$, and let all other q-oscillators be at rest. With that we arrive at a unique periodic orbit in the phase space of the FPU model. We expect that the orbit will stay localized in q-space at least up to some critical nonzero value of α (and similarly for the β-model [28]). We proceed with a series of successful numerical experiments continuing periodic orbits of the linear chain to nonzero nonlinearity. These orbits as well as their Floquet spectra can be calculated using well developed computational tools [16] for exploring periodic orbits. We choose a Poincaré section plane $\{x_s=0, \dot{x}_s>0\}$, where $s=[2(N+1)/q_0]$ corresponds to an antinode of the mode Q_{q_0}. We map the plane $\vec{y}$ (all phase variables excluding x_s) onto itself integrating the equations of motion (1) until the trajectory crosses the plane again: $\vec{y}^{n+1}=\vec{\mathcal{F}}(\vec{y}^n)$. A periodic orbit of the FPU chain corresponds to a fixed point of the generated map. As the initial guess, we use the point corresponding to the q_0th linear mode: $\dot{x}_n(0)=\sqrt{2/N+1}\dot{Q}_{q_0}(0)\sin(\pi q_0 n/N+1)$, $x_n(0)=0$. The vector function $\vec{\mathcal{G}}(\vec{y})=\vec{\mathcal{F}}(\vec{y})-\vec{y}$ is used to calculate the Newton matrix $\mathcal{N}=\partial\mathcal{G}(\vec{y})_i/\partial y_j$. We use a Gauss method to solve the equations $\vec{\mathcal{G}}(\vec{y})=\mathcal{N}\cdot(\vec{y}-\vec{y}')$ for the new iteration $\vec{y}'$ and do final

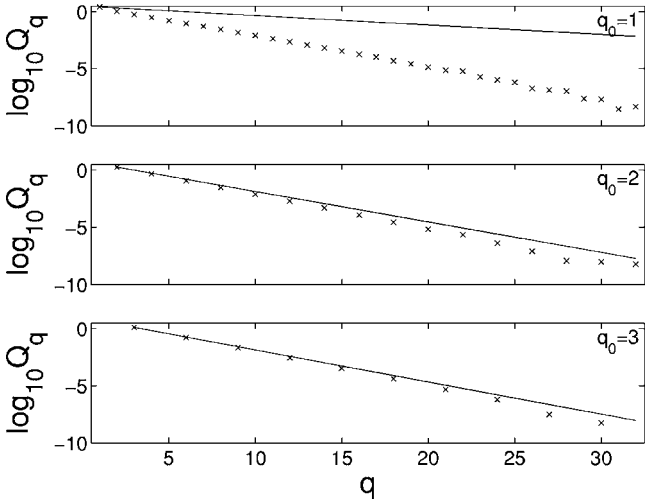

FIG. 2. Snapshots of the linear mode coordinates Q_q (symbols) along with analytical predictions (lines) for QBs with $q_0=1,2,3$ for $\alpha=0.25$, $E=0.077$, $N=32$, at the moment when all velocities $\dot{Q}_q$ equal zero. Some modes have zero contributions and their corresponding symbols are not plotted here.

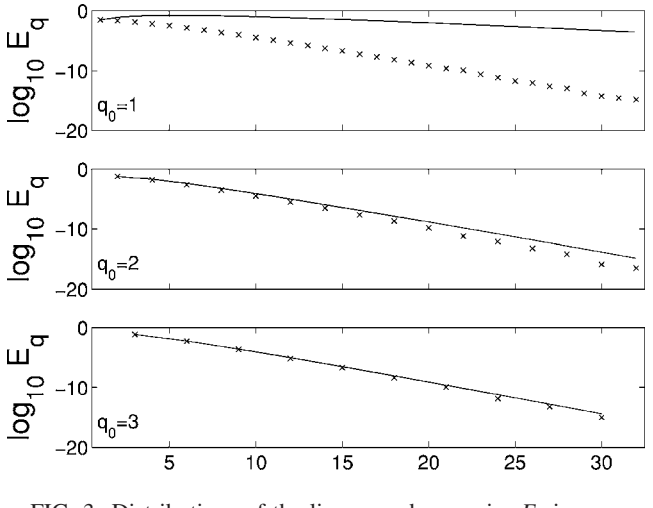

FIG. 3. Distributions of the linear mode energies E_q in q-space for QBs with $q_0=1,2,3$ for $\alpha=0.25$, $E=0.077$, $N=32$.

corrections to adjust the correct total energy E. The iteration procedure continues until the required accuracy ε is obtained: $\|\vec{\mathcal{F}}(\vec{y})-\vec{y}\|/\|\vec{y}\|<\varepsilon$ (we have varied ε from 10^{-5} to 10^{-8}), where $\|\vec{y}\|=\max\{|y_i|\}$. We also note that all periodic orbits computed here are invariant under time reversal, which means that there exist times t_0 when $Q_q(t_0+t)=Q_q(t_0-t)$ for all q. Since mode velocities vanish at these times, a QB can also be computed, e.g., by initially choosing all mode velocities to be zero, and integrating until $\dot{Q}_{q_0}$ vanishes again with the same sign of Q_{q_0} as it was at the starting point. Then the fixed point of the corresponding map of the mode coordinates only suffices to obtain an exact periodic solution.

We have used one of the original parameter sets of the FPU-α study $\alpha=0.25$, $E=0.077$, $N=32$ [1] to find stable q-localized QB solutions with most of the energy concentrated in the mode $q_0=1$ (and added the cases $q_0=2,3$ for comparison; see Figs. 2 and 3). Note that $2(N+1)$ is always a multiple of 2, and in the particular case of $N=32$ it is also a multiple of 3. Then, according to Eq. (6), for $q_0=2$ and $q_0=3$ only modes with q being a multiple of q_0 are excited. Let us discuss the properties of the found solutions in some detail. In contrast to the original FPU trajectories, the QB is characterized by mode energies being almost constant in time. The straight lines in Fig. 1 compare the mode energies on the QB with $q_0=1$ with the FPU trajectory. The period of the QB solutions is very close to the corresponding period $T_{q_0}=2\pi/\omega_{q_0}$ of the harmonic mode, which is continued. During one QB period of oscillation, a relatively small energy interchange between the modes (of the order of 2%) is observed [(Figs. 4(a)–4(c))] with frequencies that correspond to multiples of the QB frequency—just like the small fluctuations of the mode energies for the FPU trajectory mentioned above. There are well defined intervals during which the energy of nonlinear coupling energy $E_c=E_{\text{tot}}-\Sigma_{q=1}^{N}E_q$ (E_{tot} being the full energy of the chain) increases sharply, yet being overall very small [between 1 and 3% of the total energy, see Fig. 4(d)]. In Fig. 5, we show the time dependence of the first five mode coordinates on the QB with $q_0=1$. The time reversal symmetry is nicely observed (although not used for construction) at times $t_0\approx 17,49$. Note also that while Q_1 oscillates predominantly with the main QB frequency Ω_{QB}, which is close to ω_1, the second mode Q_2 is dominated by $2\Omega_{\text{QB}}$, the third one Q_3 by $3\Omega_{\text{QB}}$, etc.

We conclude the numerical results on the α-FPU case with QB solutions for $q_0=1$, $E=0.077$ and various values of α up to $\alpha=0.8$, which are shown in Fig. 6. We observe that the localization length increases with increasing α, so there is a clear tendency towards QB delocalization.

B. Estimating the localization length

To demonstrate localization of a QB solution in q-space analytically, we expand the solution to Eq. (4) into an asymptotic series with respect to the small parameter $\sigma=\alpha/\sqrt{2(N+1)}$,

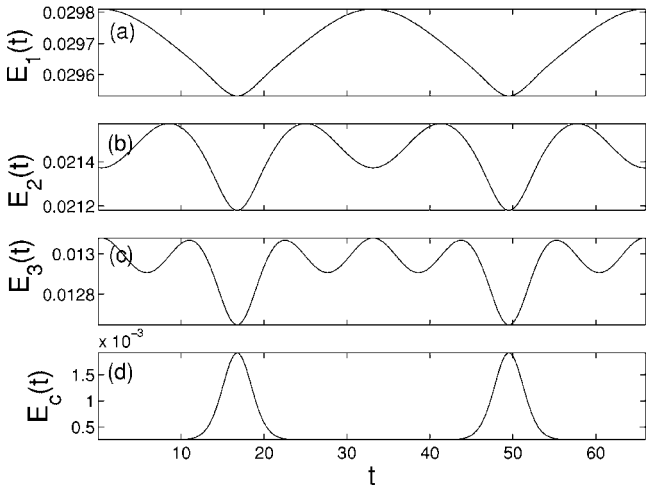

FIG. 4. Evolution of the linear mode energies (a) E_1, (b) E_2, (c) E_3, and the energy of nonlinear coupling (d) E_c (see the text for definition) for the QB with $q_0=1$, $\alpha=0.25$, $E=0.077$, $N=32$.

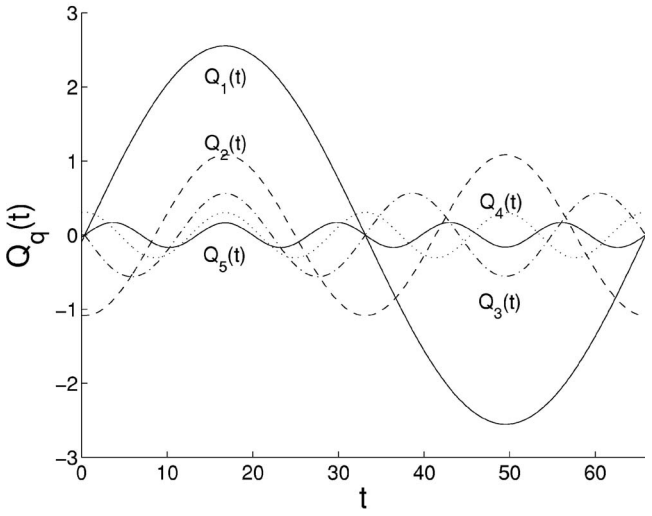

FIG. 5. Evolution of the linear mode coordinates $Q_{1,2,3,4,5}$ for the QB with $q_0=1$, $\alpha=0.25$, $E=0.077$, $N=32$.

$$Q_q(t) = \sum_{n=0}^{\infty} \sigma^n Q_q^{(n)}(t). \tag{14}$$

Inserting this expansion into Eq. (4), we obtain equations for the variables $Q_q^{(n)}(t)$. The equation for the zero order $n=0$ reads

$$\ddot{Q}_q^{(0)} + \omega_q^2 Q_q^{(0)} = 0, \tag{15}$$

and for $n>0$

$$\ddot{Q}_q^{(n)} + \omega_q^2 Q_q^{(n)} = -\omega_q \sum_{l,m=1}^{N} \omega_l \omega_m B_{qlm} \sum_{\substack{n_{1,2}=0 \\ n_1+n_2=n-1}}^{n-1} Q_l^{(n_1)} Q_m^{(n_2)}. \tag{16}$$

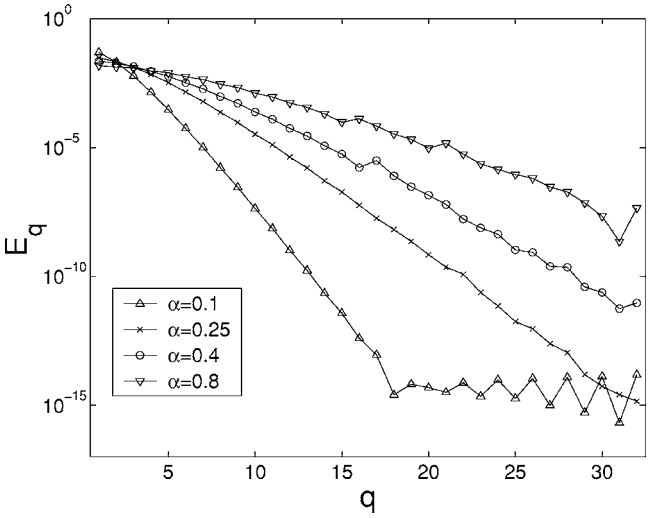

FIG. 6. Distributions of the linear mode energies E_q for $\alpha=0.1$, 0.25, 0.4, and 0.8 for QBs with $q_0=1$, $E=0.077$, $N=32$.

As the zero-order approximation, we take a single-mode solution to Eq. (15) with $Q_q^{(0)}(t) \neq 0$ only for $q=q_0$,

$$Q_q^{(0)} = \delta_{q,q_0} A_{q_0} \cos \omega_{q_0} t. \tag{17}$$

Consider the first-order equations [case $n=1$ in Eq. (16)]. The right-hand part in Eq. (16) contains only one nonzero term corresponding to $l=m=q_0$, $n_1=n_2=0$. The coefficient B_{qlm} here is nonzero only for $q=2q_0$ [here we assume $2q_0 \leqslant N$, so that the second Kronecker symbol in Eq. (6) equals zero]. Thus, in the first order the only variable different from zero is $Q_{2q_0}^{(1)}(t)$.

Similarly, for $n=2$, provided $3q_0 \leqslant N$, we get $Q_q^{(2)}(t) \neq 0$ for $q=q_0$ and $3q_0$ only; for $n=3$ and $4q_0 \leqslant N$, we obtain nonzero values at $q=2q_0$ and $4q_0$, and so on.

The above allows us to formulate the following proposition.

In the $(k-1)$th order of asymptotic expansion, provided $kq_0 \leqslant N$, variables $Q_q^{(k-1)}(t)$ differ from zero only for $q=\theta q_0, (\theta+2)q_0, \ldots, (k-2)q_0, kq_0$,

$$Q_q^{(k-1)}(t) = 0 \quad \forall\, q \notin \{\theta q_0, (\theta+2)q_0, \ldots, (k-2)q_0, kq_0\}, \tag{18a}$$

where $\theta=1$ for odd k and $\theta=2$ for even k.

It means that the first nonzero expansion term for a mode $q=kq_0$ is of the order $k-1$,

$$Q_{kq_0}^{(m)}(t) = 0 \quad \forall\, m < k-1. \tag{18b}$$

In Appendix B, we prove this statement by the method of mathematical induction and approximate the first nonzero term for a mode $q=kq_0$ at $kq_0 \ll N$,

$$Q_{kq_0}^{(k-1)}(t) = A_{kq_0}\{\cos k\omega_{q_0} t + O[(kq_0/N)^2]\}, \tag{19a}$$

where

$$A_{kq_0} = \frac{A_{q_0}^k}{\omega_{q_0}^{k-1}}. \tag{19b}$$

Ignored expansion terms lead to shifting the QB orbit frequency and next-order corrections to its shape.

Multiplying Eq. (19) by σ^{k-1} and inserting it into Eq. (9), we approximate the mode energies as

$$E_{kq_0} = k^2 \gamma^{k-1} E_{q_0}\{1 + O[(kq_0/N)^2]\}[1 + O(\sigma)], \tag{20a}$$

where

$$\gamma = \frac{\alpha^2 (N+1)^3 E_{q_0}}{\pi^4 q_0^4}. \tag{20b}$$

Note that although the mode energies are not strictly conserved in time, their variation is small, being limited to the orders of magnitude indicated in Eq. (20a) in parentheses (cf. Fig. 4). We arrive at an exponential decay in q-space dressed with a power law,

$$\ln(E_q) = 2\ln\left(\frac{q}{q_0}\right) + \frac{q}{q_0}\ln\gamma + \ln\left(\frac{E_{q_0}}{\gamma}\right) \tag{21}$$

with exponent $q_0^{-1}\ln\gamma$ for the exponential part. The predicted decay (20) fits nicely with a computed QB with $q_0=1$ and $\alpha=0.025$ as shown in Ref. [14]. In Figs. 2 and 3 we compare Eq. (20) with the numerical results for $\alpha=0.25$ and $q_0=1,2,3$. While q_1 shows that the analytical results underestimate the degree of localization with increasing α, we note that it does even at these values α better for larger values of q_0.

The calculation described is expected to fail at γ close to or greater than 1, when Eq. (20) does not support q-space localization. At the same time the comparison with the numerical results shows that higher-order corrections to the analytical decay law extend the region of QB localization. Thus we estimate a lower bound for the QB delocalization threshold energy E^{loc} as

$$E^{\mathrm{loc}} = \pi^4\alpha^{-2}(N+1)^{-3}q_0^4. \tag{22}$$

The scaling behavior is in good agreement with an analytical estimation of the resonance threshold in the α-model due to second-order nonlinear resonance overlap, suggested in Ref. [9], which reads $\alpha^2 EN^3 \approx q_0^4$.

Finally, we stress an even closer relation between the localization of q-breathers within the used perturbation theory and the Fourier series convergence of analytic periodic functions (11)–(13). One arrives from the QB problem to these equations by simply assuming $\omega_q=\mathrm{const}$.

C. Stability of q-breathers in the α-FPU system

An important problem is the stability of QBs. For computing linear stability of an orbit $\hat{Q}_q(t)$, the phase space flow around it is linearized by making a replacement

$$Q_q = \hat{Q}_q(t) + \xi_q \tag{23}$$

in the equations of motion (5) and subsequent linearizing the resulting equations with respect to ξ_q. Orbit stability is then characterized by the eigenvalues of the Floquet matrix, which defines the linear transformation of small deviations ξ_q by the linearized equations over one period of the orbit. If all eigenvalues μ_j have the absolute value 1, the orbit is stable, otherwise it is unstable [16,17].

All QB solutions presented in this section are linearly stable, i.e., all eigenvalues of the Floquet matrix which characterize the linearized phase space flow around the QB orbits reside on the unit circle. This is at variance with the case of the β-FPU model, which will be discussed below [29].

V. β-FPU SYSTEM

A. Numerical results

Launching an FPU trajectory by exciting a single low-frequency mode leads to similar observations as for the α-model. Again energy is localized in q-space on a few modes, sometimes coined natural packets [30], which again persists for very long times.

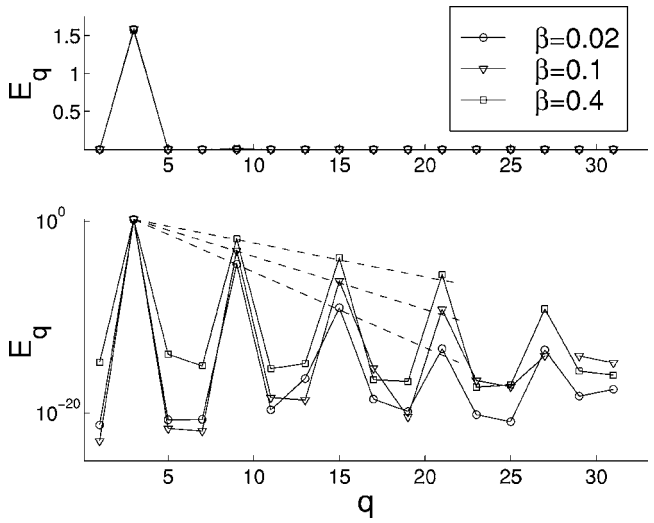

FIG. 7. Energy distributions between q-modes in QBs for different nonlinear coupling coefficients β vs q in linear and log scales with analytical estimations of the QBs exponential localization (dashed lines). Parameters are $E=1.58$, $q_0=3$, $N=32$. Only odd modes are shown (see text). The symbols for $q\neq 3,9,15,21,27$ represent upper bounds, the real mode energies might be even less. Note that QBs persist even far beyond the stability threshold (see Fig. 8).

It is possible to construct QBs in the β-FPU model, following the same way as described above for the α-model.

For numerical calculations, we use a modified scheme. The section plane is defined in the q-space as $\{Q_{q_0}=0, \dot{Q}_{q_0}>0\}$. It is parametrized as $\vec{r}\equiv\{\dot{Q}_q, q\neq q_0\}$. The even coupling potential and fixed boundary conditions enable us to introduce an additional constraint $Q_q(t=0)=0$, and the velocity $\dot{Q}_{q_0}$ is obtained using the condition of energy conservation $\dot{Q}_{q_0}(t=0)=\sqrt{2E-\Sigma_{q\neq q_0}\dot{Q}_q^2(t=0)}$. As in the case of the α-model, the QB is searched as a fixed point of the mapping $\vec{r}^{n+1}=\vec{\mathcal{F}}(\vec{r}^n)$.

We obtain QBs that are exponentially localized in q-space (Fig. 7). The smaller β is, the faster is the decay of the energy distribution with increasing wave number q. Note that due to the parity symmetry of the β-model [Eq. (2) is invariant under $x_n\rightarrow -x_n$ for all n] only odd q-modes are excited by the $q_0=3$ mode and get coupled [31]. This follows also from the coupling matrix (7).

B. Estimating the localization length

In the analytical computation, the solution to Eq. (5) is expanded in powers of a small parameter $\rho=\beta/2(N+1)$. In the nth order of expansion, variables $Q_q^{(n)}$ differ from zero at $q=q_0,3q_0,\ldots,(2n+1)q_0$ only. Then the first nonzero expansion term for a mode $(2n+1)q_0$ is of the order n. Using the same approach of mathematical induction as described in Appendix B, mode energies in a QB are approximated as follows:

$$E_{(2k+1)q_0} = \lambda^k E_{q_0}(1+O\{[(2k+1)q_0/N]^2\})[1+O(\rho)], \tag{24a}$$

where

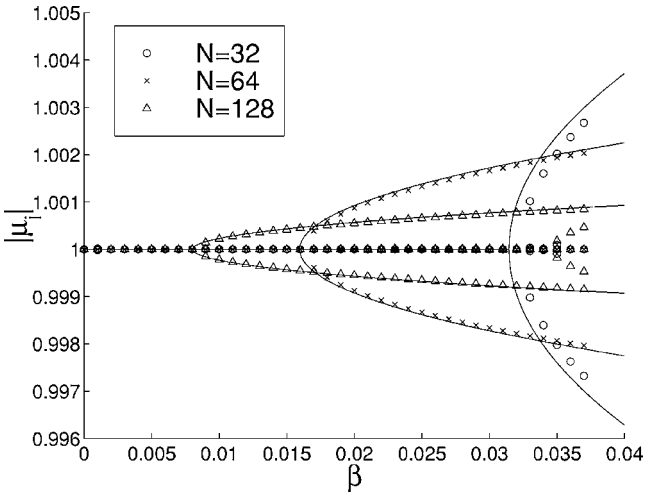

FIG. 8. Absolute values of Floquet multipliers $|\mu_i|$ of QBs with the energy $E=1.58$ and $q_0=3$ and different N vs β. Symbols: numerical results, lines: analytical results.

$$\lambda = \frac{9\beta^2 E_{q_0}^2 (N+1)^2}{64\pi^4 q_0^4}. \tag{24b}$$

Again, time variation of the mode energies is limited to the orders of magnitude indicated in Eq. (24a). We arrive at a pure exponential decay

$$\ln(E_q) = \ln E_{q_0} + \frac{1}{2}\left(\frac{q}{q_0} - 1\right)\ln\lambda \tag{25}$$

with the exponent $(2q_0)^{-1}\ln\lambda$. The predicted decay (24) fits nicely with the computed QBs in Fig. 7.

The QB delocalization threshold is then estimated as

$$E_{q_0} = \frac{8}{3}\pi^2 q_0^2 \beta^{-1}(N+1)^{-1}. \tag{26}$$

The scaling behavior is in good agreement with an analytical estimation of the resonance threshold in the β-model due to second order nonlinear resonance overlap, obtained in Ref. [9], which reads $\beta EN \approx q_0^2$.

C. Stability of q-breathers for the β-FPU model

First, we study QB stability by computing the Floquet matrix numerically and diagonalizing it. In Fig. 8, we plot the absolute values of the Floquet eigenvalues of the computed QBs versus β for different system sizes N. QBs are stable for sufficiently weak nonlinearities (all eigenvalues have absolute value 1). When β exceeds a certain threshold, two eigenvalues get absolute values larger than unity (and, correspondingly, another two get absolute values less than unity) and a QB becomes unstable. Remarkably, unstable QBs can be traced far beyond the stability threshold, and, moreover, they retain their exponential localization in q-space (Fig. 7). As β is increased further, new bifurcations of the same type are observed.

To study QB stability analytically in the first-order approximation, we write down the QB solution in the form

$$\hat{Q}_q(t) = \delta_{qq_0} A\cos\hat{\omega}t + O(\rho), \tag{27}$$

where $\hat{\omega}$ is the QB frequency, slightly shifted from ω_{q_0} due to nonlinearity. The residual term $O(\rho)$ includes corrections to the QB orbit shape by expansion terms of order 1 and higher.

The first-order correction to the QB frequency is determined by secularity caused by resonant nonlinear self-forcing of the mode q_0 in the first order of expansion,

$$\ddot{Q}_{q_0}^{(1)} + \omega_{q_0}^2 Q_{q_0}^{(1)} = -3\omega_{q_0}^4 Q_{q_0}^{(0)3}. \tag{28}$$

This equation is identical to that of an isolated oscillator with cubic nonlinearity (Duffing oscillator). The well-known expression of nonlinear frequency shifting in the Duffing oscillator then yields

$$\hat{\omega} = \omega_{q_0}\left(1 + \frac{9\beta E_{q_0}}{8(N+1)} + O(\rho^2)\right). \tag{29}$$

Linearizing equations of motion (5) around Eq. (27) according to Eq. (23), we arrive at a Mathieu equation (see Appendix C), which finally leads to an estimation of the Floquet multipliers, which leave the unit circle due to a primary parametric resonance and cause instability,

$$|\mu_{j_1 j_2}| = 1 \pm \frac{\pi^3}{4(N+1)^2}\sqrt{R - 1 + O\left(\frac{1}{N^2}\right)}, \tag{30}$$

where

$$R = 6\beta E_{q_0}(N+1)/\pi^2. \tag{31}$$

The bifurcation occurs at $R=1+O(1/N^2)$. This instability threshold coincides with the criterion of transition to weak chaos reported by De Luca *et al.* [8]. Note that Eq. (30) does not contain the principal mode number q_0. Below the stability threshold (except for possible small high-order resonance zones), a set of stable QB modes exists. In the thermodynamical limit $N\to\infty$, however, the energy of stable QBs tends to zero. Note that according to our analytical (Appendix C) and numerical results, the instability modes correspond to $q'=q_0\pm 1$ and are even modes if q_0 is odd and vice versa. The observed instability is thus connected to a lowering of the symmetry compared to the higher symmetry QB. That has been also observed to be the driving pathway for the onset of low-dimensional stochasticity in the FPU trajectory at the weak chaos transition [8,32], when the FPU trajectory acquires chaotic components in the time evolution, while still being localized in q-space.

The result (30) is plotted in Fig. 8 with solid lines for $N=32$, 64, and 128, demonstrating good agreement with the numerical results. The agreement improves with increasing N [33].

Driscoll and O'Neil studied the instability of a single soliton in the continuum mKdV limit of the β-FPU model [34] with periodic boundary conditions. A stability threshold obtained within the mKdV equation will qualitatively or semiquantitatively agree with the correct value obtained for the discrete chain, if the instability sets in for QBs that do not contain significant short-wave-length components. The relation between the stability of a single soliton and a QB is less

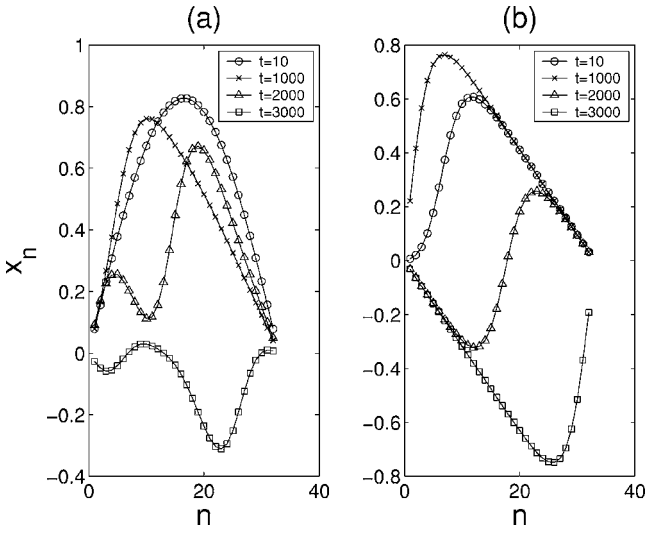

FIG. 9. Snapshots of displacements (a) of the original FPU trajectory for $\alpha=0.25$, $E=0.077$, $N=32$ [1] and (b) of the corresponding exact QB solution from Fig. 2 taken at different times.

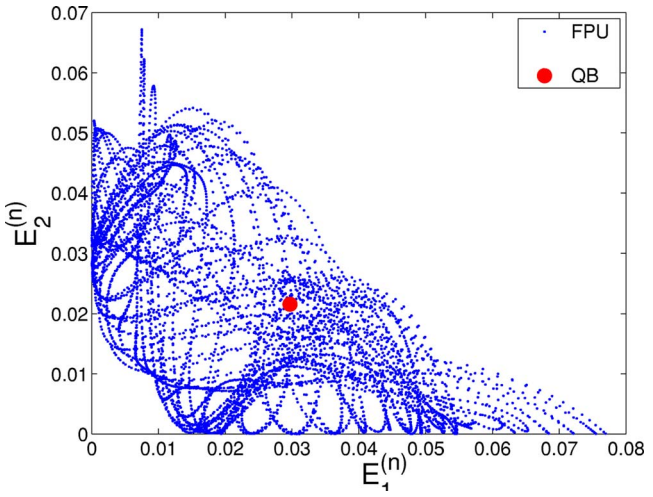

FIG. 10. (Color online) Map of the mode energies E_1 and E_2 on the FPU trajectory after consecutive periods of the corresponding q-breather for $N=32$, $\alpha=0.25$, and $q_0=1$. The thick dot is the results for the QB orbit.

clear, since in the limit of vanishing nonlinearity QBs in chains or field equations with periodic boundary conditions correspond to standing waves, while single solitons transform into plane (running) waves.

We conclude this section with the observation that the stability (31) and delocalization (26) threshold estimates for QBs contain a unique parameter βEN where E is the total energy, at variance with scaling estimates for the transition times to equipartition [35], which obtain $\beta E/N$ instead.

VI. QBS AND THE FPU-TRAJECTORY FOR THE α-FPU MODEL

Departing from the QB orbit in phase space in the direction of the initial condition of the FPU trajectory implies adding to the QB solution (which is localized in q-space) a perturbation, which is localized in q-space as well. The perturbed trajectory will evolve essentially on a low-dimensional torus in phase space, whose dimension will correspond to the number of modes excited on the QB orbit, e.g., for $\alpha=0.25$ and $q_0=1$ about four or five. In Fig. 9, we compare snapshots of displacements at different times obtained for the original FPU trajectory in Ref. [1] and for the numerically exact QB solution from Fig. 2 for $\alpha=0.25$ and observe similar evolution patterns (see also Ref. [12]). Moreover, we took a series of points on a line that connected initial conditions of the FPU trajectory ($E_{q\neq 1}=0$) with the numerically exact QB solution from Fig. 2. For each of these points, we integrated the corresponding trajectory and measured the average deviation Δ from the QB orbit. The dependence of Δ on the line parameter turns out to be an almost linear one, starting from zero when being very close to the QB orbit, and ending with a maximum value when being close to the FPU trajectory. That supports the expectation that the FPU trajectory is a perturbation of the QB orbit. The FPU recurrence is gradually appearing with increasing Δ and is thus directly related to the regular motion of a slightly perturbed QB periodic orbit, which we tested also numerically. In Fig. 10, we plot the mode energies E_1 and E_2 during integration of the FPU trajectory for $\alpha=0.25$ and $q_0=1$ after consecutive periods of the q-breather solution. The regular pattern indicates regular motion, and the thick dot, which corresponds to the q-breather solution itself, resides inside the quasiperiodic cloud of the FPU trajectory, indicating once more that the FPU trajectory is a perturbation of the q-breather and evolves around the QB in phase space. Zooming the time dependence of the mode energies for the FPU trajectories on time scales comparable to the QB period shows very similar nearly periodic fluctuations as in Fig. 4 that are generated by the QB period. Using the linearized phase space flow around a QB, we can estimate an effective recurrence time, which for the original FPU case is two times smaller than the recurrence time for the FPU trajectory. We tracked the change of the recurrence time with increasing Δ. When coming closer to the FPU trajectory, simply every second recurrence as observed for small deviations from the QB is suppressed, leaving us with the FPU recurrence time. That effect may be due to additional nonlinear contributions to the phase space flow around a QB.

Finally, we note that extremely long computations of the FPU trajectory have been reported recently [36]. The trajectory localizes in q-space (and thus stays close to a q-breather) for times up to 10^{10}. Only after that is a mixing of mode energies observed, possibly due to Arnold diffusion. Notably, the critical time has been estimated by numerical scaling analysis for shorter transition times [12].

VII. TOWARD TRANSIENT PROCESSES AND THERMAL EQUILIBRIUM

Once the existence and stability of QBs as exact solutions are established, it is interesting to analyze the contribution of these trajectories to the dynamics of transient processes and thermal equilibrium. It is well known that in states corre-

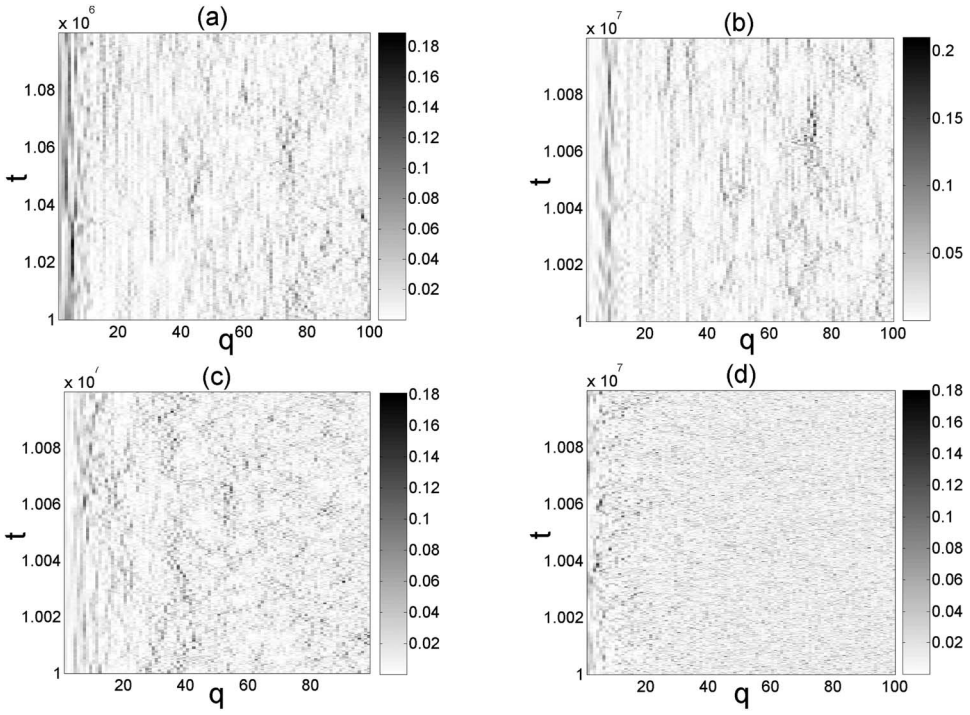

FIG. 11. Space-time plots of mode energies E_q evolving from the initial localization in the third mode for $N=100$, $E_3(0)=1.58$, and (a) $\beta=0.6$, $T_{\mathrm{tr}}=10^6$; (b) $\beta=0.6$, $T_{\mathrm{tr}}=10^7$; (c) $\beta=1.25$, $T_{\mathrm{tr}}=10^7$; (d) $\beta=5.0$, $T_{\mathrm{tr}}=10^7$.

sponding to energy equipartition between degrees of freedom (or thermal equilibrium), energy distribution demonstrates strong statistical properties, with no energy concentrations on average in some subparts of phase space. This circumstance, however, does not preclude the existence of finite-time energy localizations whose lifetime may substantially exceed the characteristic period of plane waves. We recall the studies of discrete breather contributions to the dynamics of nonlinear lattices in thermal equilibrium and transient processes [37].

Here we present results of numerical simulations of the β-FPU chain ($N=100$, fixed boundary conditions) with two types of initial conditions: (i) all energy is located in a single mode $E_{\mathrm{tot}}=E_3=1.58$, $E_{q\neq 3}=0$, (ii) all energy is randomly distributed among all modes: $Q_q(0)=\xi_k/\omega_q$, $\dot{Q}_q(0)=\eta_k$, where ξ_k, η_k are random numbers, uniformly distributed in $[-c,c]$, c taken to ensure $E_{\mathrm{tot}}/N=0.2$.

In the first case, we take three values of $\beta=0.6,1.25,5.0$, for which energy delocalizes and essentially redistributes among the degrees of freedom after some transition time T_{tr} (Fig. 11). We note that with the chosen values of q_0, E_0, N our previous results suggest that the QB becomes unstable at $\beta\approx 0.01$ and delocalizes at $\beta\approx 1.6$. The figures show a time window width 10^5, which is much larger than the largest QB periods, which are of the order of 400.

We observe that stochastic motion and energy flow to higher modes lead the system into a possibly long transient regime, in which QB-like objects (finite-lifetime single-mode excitations) are observed for all q [Figs. 11(a) and 11(b)]; note that at different T_{tr}, qualitatively the same picture is observed]. These objects survive for up to a hundred periods of phonon band oscillations. Since the smallest chosen values for β exceed the QB instability threshold value, we conclude that the QB instability is of local character in q-space and does not carry a perturbed trajectory far away. When β is increased, the lifetime of higher-frequency QBs drops down and they disappear in the high- and middle-frequency regions [Fig. 11(c), $\beta=1.25$] and then remain observable only in the few lowest modes [Fig. 11(d), $\beta=5.0$]. Note that for these values of β we already exceed the delocalization threshold estimate for QBs. The observation of surviving low-q QB-like structures suggests that the energy flow between low- and high-q modes is sufficiently weak, so that some excess of energy is transferred into the large-q domain, allowing for long-time energy localization in the low-q domain.

Similar effects can be observed for the second type of initial conditions (Fig. 12), which mimics thermal equilibrium. At low β, QBs can be observed in the whole phonon band frequency domain [Figs. 12(a) and 12(b), $\beta=0.05$]. As β is increased, high- and medium-frequency QBs disappear [Figs. 12(c) and 12(d), $\beta=0.1,0.4$]. Note that by rescaling coordinates and momenta (and hence energies), the set of total energies and nonlinear coupling strengths for both types of initial conditions practically coincide, so one may directly compare all subfigures from Figs. 11 and 12.

VIII. CONCLUSION

We report on the existence of q-breathers as exact time-periodic low-frequency solutions in the nonlinear FPU system. These solutions are exponentially localized in the q-space of the normal modes and preserve stability for small enough nonlinearity. They continue from their trivial counterparts for zero nonlinearity at finite energy. The stability threshold of QB solutions coincides with the weak chaos threshold in Ref. [8]. The delocalization threshold estimate of QBs shows identical scaling properties as the estimate of equipartition from second-order nonlinear resonance overlap [9]. Persistence of exact stable QB modes is shown to be

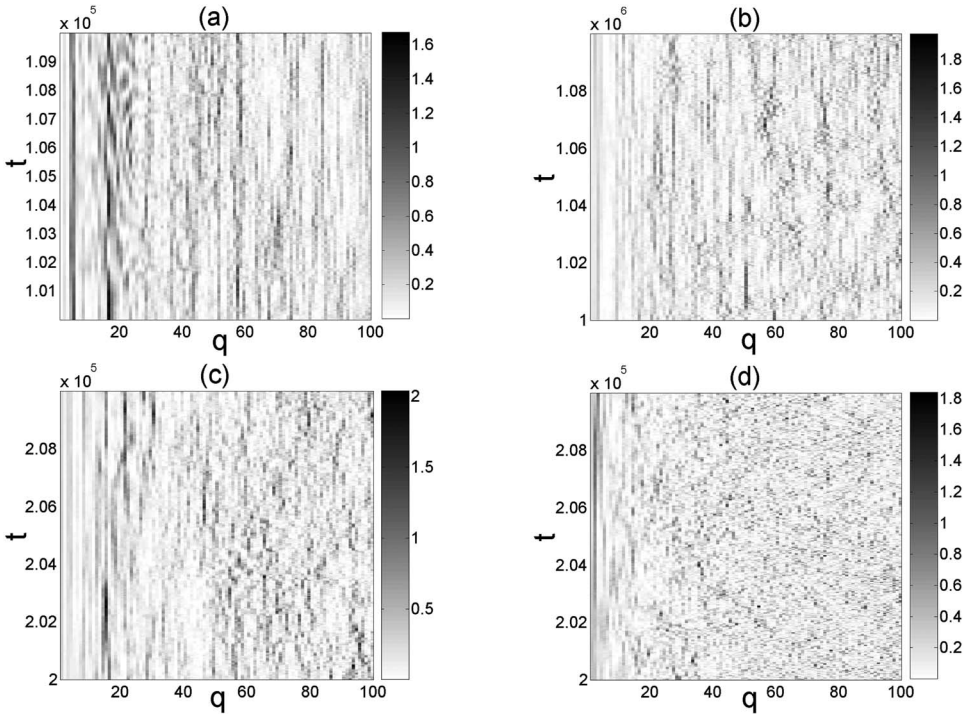

FIG. 12. Space-time plots of mode energies E_q evolving from random initial conditions for $N=100$, $E_{\mathrm{tot}}/N=0.2$, and (a) $\beta=0.05$, $T_{\mathrm{tr}}=10^5$; (b) $\beta=0.05$, $T_{\mathrm{tr}}=10^6$; (c) $\beta=0.1$, $T_{\mathrm{tr}}=2\times10^5$; (d) $\beta=0.4$, $T_{\mathrm{tr}}=2\times10^5$.

related to the FPU observation. The FPU trajectories computed 50 years ago are perturbations of the exact QB orbits. Remarkably, localization in q-space persists even for parameters when the QBs become unstable. The QB concept—tracing time-periodic and q-space localized orbits together with their stability and degree of localization—allows us to explain qualitatively and semiquantitatively many aspects of the 50-year-old FPU problem. Moreover, we show that dynamical localization in q-space persists for transient processes and thermal equilibrium remarkably well. Note that for certain cases, specific symmetries allow us to obtain q-breathers with compact localization [31,38], where they have been interpreted as anharmonic plane-wave solutions.

The concept of QBs and their impact on the evolution of excitations in the FPU system is expected to apply far beyond the stability threshold of the QB solutions reported in the present work. Generalizations to higher-dimensional lattices and other Hamiltonians are straightforward, due to the weak constraint imposed by the nonresonance condition needed for continuation. QBs can also be expected to contribute to peculiar dynamical features of nonlinear lattices in thermal equilibrium, e.g., the anomalous heat conductivity in FPU lattices [3]. Another interesting problem is the change from fixed to periodic boundary conditions. In most cases such as the above-considered FPU chain, this will cause twofold degeneracies of the normal mode spectrum. Consequently, both standing and traveling waves can be considered as potential QB candidates when adding nonlinearity. Yet one has to cope with the above-mentioned degeneracy and understand its impact.

A quantization of QBs will lead straightforwardly to quantum QBs, which will not differ much from their classical counterparts, due to the absence of discrete symmetries that may lead to tunneling effects. Thus a quantum QB state will be localized in q-space pretty much as a classical QB, allowing for ballistic-type excitations in the low-q domain.

Finally, we remark that the QB concept is not even constrained to an underlying lattice in real space. What we need in order to construct a QB is a discrete spectrum of mode energies, and nonlinearity that induces mode-mode interactions. Thus QBs can be constructed in various nonlinear field equations on a finite spatial domain as well, since one again obtains in the limit of small amplitudes a discrete mode spectrum, with the only difference from a finite lattice being that the number of modes is infinite.

ACKNOWLEDGMENTS

We thank T. Bountis, S. Denisov, F. Izrailev, Yu. Kosevich, A. J. Lichtenberg, P. Maniadis, K. Mishagin, T. Penati, V. Shalfeev, and W. Zakrzewski for stimulating discussions. M.I. and O.K. appreciate the warm hospitality of the Max Planck Institute for the Physics of Complex Systems. M.I. and O.K. also acknowledge support of the "Dynasty" Foundation.

APPENDIX A: CONTINUATION OF QBS FROM ZERO TO NONZERO α

We introduce a Poincaré section S [39] defined by $\{P_{q_0}=0, Q_{q_0}>0\}$. Let S be parametrized by a vector $\boldsymbol{s}$, whose components are all variables of state except P_{q_0}. We denote the coordinates and momenta of all oscillators except q_0 as a vector $\boldsymbol{r}$ of length $2N-2$,

$$\boldsymbol{r}=\{Q_1,P_1,\ldots,Q_{q_0-1},P_{q_0-1},Q_{q_0+1},P_{q_0+1},\ldots,Q_N,P_N\}.$$

Then $\boldsymbol{s}$ consists of all components of $\boldsymbol{r}$ and the coordinate Q_{q_0}.

In the trivial case of decoupled modes ($\alpha=0$) at any given q_0, there exists a family of periodic orbits corresponding to various values of the amplitude A of the q_0th oscillator with all the others being at rest. Each of these orbits crosses S at a point $\boldsymbol{s}_A$ with $\boldsymbol{r}=0$, $Q_{q_0}=A>0$. Let us pick one of these orbits by choosing a value of A and consider the Poincaré mapping [39] of a vicinity of $\boldsymbol{s}_A$ into S. Then $\boldsymbol{s}_A$ is a fixed point of this map. Taking into account the dependence of the mapping on α, we write it down in the form of a vector function

$$\bar{\boldsymbol{s}} = \boldsymbol{F}(\boldsymbol{s};\alpha) = \boldsymbol{F}(\boldsymbol{r}, Q_{q_0};\alpha). \tag{A1}$$

We recall that a Poincaré mapping is C^1 [39].

In order to apply the implicit function theorem to continue the fixed point (and thus the periodic orbit) to the case of nonzero α, we need to eliminate the degeneracy caused by energy conservation. For this we consider a mapping of the space $\mathbb{R}^{2N-2}$ of vectors $\boldsymbol{r}$ onto itself obtained by fixing the value of Q_{q_0} in the map (A1) at the constant quantity A,

$$\bar{\boldsymbol{r}} = \boldsymbol{G}(\boldsymbol{r};\alpha), \quad \text{where } G_j(\boldsymbol{r};\alpha) = F_j(\boldsymbol{r}, A;\alpha), \quad j=\overline{1,2N-2}. \tag{A2}$$

Note that a fixed point of the mapping (A2) can be uniquely associated with a fixed point of the Poincaré mapping (A1) and, thus, with a periodic orbit. Indeed, the coordinate Q_{q_0} in the end point of the mapping trajectory can be expressed as a function of $\boldsymbol{r}$ using the energy conservation condition $H(\{Q_q,P_q\})=E$, where E is the energy in the starting point and H is the Hamiltonian, since $\partial H/\partial Q_{q_0}\neq 0$ in this point. So, if $\boldsymbol{r}$ is a fixed point of Eq. (A2), then the corresponding vector $\boldsymbol{s}$ (including the coordinate $Q_{q_0}=A$) is a fixed point of Eq. (A1).

A fixed point of Eq. (A2) is a root of the equation

$$\boldsymbol{Z}(\boldsymbol{r};\alpha) = \boldsymbol{0}, \quad \text{where } \boldsymbol{Z}(\boldsymbol{r};\alpha) = \boldsymbol{G}(\boldsymbol{r};\alpha) - \boldsymbol{r}. \tag{A3}$$

Since $\boldsymbol{s}_A$ is a fixed point of Eq. (A1) at $\alpha=0$, we get $\boldsymbol{Z}(0,0)=0$. As the map $\boldsymbol{F}$ is C^1, $\boldsymbol{Z}$ is also C^1, and we can apply the implicit function theorem to express $\boldsymbol{r}$ as a function of α in some finite vicinity of the point $\alpha=0$, if the Jacobian $|\partial \boldsymbol{Z}/\partial \boldsymbol{r}|$ at $\boldsymbol{r}=0$, $\alpha=0$ is nonzero. Let us show that this is the case, provided the nonresonance condition (10) is fulfilled.

For the Jacobian, we obtain

$$\left|\frac{\partial Z_i}{\partial r_j}\right| = \left|\frac{\partial M_i}{\partial r_j} - \delta_{ij}\right| = \left|\frac{\partial F_i}{\partial r_j} - \delta_{ij}\right|, \quad i,j=\overline{1,2N-2}. \tag{A4}$$

Here $|\partial F_i/\partial r_j|$ is the monodromy matrix of the orbit, from which the row and the column corresponding to Q_{q_0} are removed. For $\alpha=0$, $\boldsymbol{r}=0$, it consists of $N-1$ noninteracting blocks

$$\begin{pmatrix} \cos\vartheta_q & \dfrac{1}{\omega_q}\sin\vartheta_q \\ -\omega_q\sin\vartheta_q & \cos\vartheta_q \end{pmatrix} \tag{A5}$$

aligned along the diagonal, each describing a rotation in the plane Q_q,P_q. Here $\vartheta_q=2\pi\omega_q/\omega_{q_0}$. The determinant of the matrix $|\partial Z_i/\partial r_j|$ is then the product of the determinants of the difference of (A5) and the identity matrix.

As long as Eq. (10) is fulfilled, none of ϑ_q equals $2\pi n$, thus none of the mentioned determinants equals zero, and the whole Jacobian $|\partial Z_i/\partial r_j|$ is nonzero.

Then, finally, the conditions of the implicit function theorem are fulfilled, and the solution to Eq. (A3) (and, thus, the QB orbit) is continued to nonzero α. Note that the same procedure is easily extendable to the β-model and other cases.

APPENDIX B: QB LOCALIZATION IN THE α-FPU MODEL

First, we note that Eqs. (18) and (19) are true for $k=1$, according to Eq. (17). Further, we assume it is true for $k=1,\ldots,n-1$ and prove that it is then true for $k=n$ as well.

Equation (16) for the order $n-1$ can be written as

$$\ddot{Q}_q^{(n-1)} + \omega_q^2 Q_q^{(n-1)} = -\omega_q \sum_{\substack{n_{1,2}=1 \\ n_1+n_2=n}}^{n-1} \sum_{l,m=1}^{N} \omega_l\omega_m B_{qlm} Q_l^{(n_1-1)} Q_m^{(n_2-1)}. \tag{B1}$$

Consider for which mode numbers q the right-hand part in Eq. (B1) is nonzero. As $n_{1,2}<n$, we obtain from Eq. (18a) $Q_l^{(n_1-1)}\neq 0$ for $l=\theta_1 q_0,\ldots,(n_1-2)q_0,n_1q_0$ only, and $Q_m^{(n_2-1)}\neq 0$ for $m=\theta_2 q_0,\ldots,(n_2-2)q_0,n_2q_0$ only, where $\theta_{1,2}$ equals 1 or 2 for $n_{1,2}$ being odd or even, respectively.

According to the definition of B_{qlm} (6) and taking into account that $nq_0\leqslant N$, we obtain $B_{qlm}\neq 0$ for $q=l+m$ and $q=|l-m|$. Then, the maximal mode number q, for which the right-hand part in Eq. (B1) is nonzero, equals $q_{\max}=n_1q_0+n_2q_0=nq_0$. The set of nonzero modes in this order of expansion is $q=\theta q_0,\ldots,(n-2)q_0,nq_0$, where θ equals 1 or 2 for odd or even n, respectively. This is equivalent to Eq. (18a) at $k=n$, which concludes the induction for Eq. (18).

To prove Eq. (19), we write down Eq. (B1) for $q=nq_0$,

$$\ddot{Q}_{nq_0}^{(n-1)} + \omega_{nq_0}^2 Q_{nq_0}^{(n-1)} = -\omega_{nq_0} \sum_{\substack{n_{1,2}=1 \\ n_1+n_2=n}}^{n-1} \omega_{n_1}\omega_{n_2} Q_{n_1q_0}^{(n_1-1)} Q_{n_2q_0}^{(n_2-1)}. \tag{B2a}$$

Here we have taken into account that the only nonzero term of the sum over l and m corresponds to $l=n_1q_0$, $m=n_2q_0$, and that $B_{nq_0,n_1q_0,n_2q_0}=1$.

As $n_{1,2}<n$, the variables $Q_{n_1}^{(n_1-1)}$ and $Q_{n_2}^{(n_2-1)}$ are expressed via Eq. (19a). Then Eq. (B2a) becomes a forced harmonic oscillator equation with a set of cosinusoidal harmonics in the right-hand part,

$$\ddot{Q}_{nq_0}^{(n-1)} + \omega_{nq_0}^2 Q_{nq_0}^{(n-1)} = \sum_{m=0}^{n} C_m \cos m\omega_{q_0} t, \tag{B2b}$$

where C_m are amplitudes of the harmonics.

Omitting the free-motion part of the solution, we write down the expression for the forced oscillations of $Q_{nq_0}^{(n-1)}$,

$$Q_{nq_0}^{(n-1)} = \sum_{m=0}^{n} \frac{C_m}{\omega_{nq_0}^2 - m^2\omega_{q_0}^2} \cos m\omega_{q_0} t. \tag{B3}$$

Note that the resonance denominator in Eq. (B3) is minimal at $m=n$. In other words, driving frequency $n\omega_{q_0}$ is the closest to the resonance among all the harmonics. Expanding the sine function in Eq. (8) into a Taylor series as $\sin x = x - x^3/6 + O(x^5)$, we approximate the mode frequencies as

$$\omega_q^2 = 4\left\{(q\varkappa)^2 - \frac{1}{3}(q\varkappa)^4 + O[(q\varkappa)^6]\right\}, \tag{B4}$$

where

$$\varkappa = \frac{\pi}{2(N+1)} \to 0.$$

The mentioned minimal denominator is then expressed at $nq_0/N \to 0$ as follows:

$$\omega_{nq_0}^2 - n^2\omega_{q_0}^2 = -\frac{1}{12}n^2(n^2-1)\omega_{q_0}^4 + O\left[\left(\frac{nq_0}{N}\right)^6\right]. \tag{B5}$$

At the same time, the relation of this denominator to any other one with $m \neq n$ is estimated as

$$\frac{\omega_{nq_0}^2 - n^2\omega_{q_0}^2}{\omega_{nq_0}^2 - m^2\omega_{q_0}^2} = O\left[\left(\frac{nq_0}{N}\right)^2\right], \quad m \neq n. \tag{B6}$$

It means that the harmonic $m=n$ dominates in the solution (B3), while all the other harmonics are small values of the order $O[(nq_0/N)^2]$ with respect to this dominating one.

Thus, Eq. (B3) can be rewritten as

$$Q_{nq_0}^{(n-1)} = \frac{12C_n}{n^2(n^2-1)\omega_{q_0}^4} \cos n\omega_{q_0} t\left\{1 + O\left[\left(\frac{nq_0}{N}\right)^2\right]\right\}. \tag{B7}$$

Inserting Eq. (19a) (valid as $n_{1,2} < n$) into Eq. (B2a), we obtain the following expression for the nth harmonic amplitude C_n in Eq. (B2b):

$$C_n = -\omega_{nq_0} \sum_{\substack{n_{1,2}=1 \\ n_1+n_2=n}}^{n-1} \omega_{n_1}\omega_{n_2}\frac{1}{2}A_{n_1q_0}A_{n_2q_0}\left\{1 + O\left[\left(\frac{nq_0}{N}\right)^2\right]\right\}. \tag{B8}$$

Inserting Eq. (B8) into Eq. (B7) and taking into account Eq. (B4), we arrive at

$$Q_{nq_0}^{(n-1)} = A_{nq_0}\left\{\cos n\omega_{q_0} t + O\left[\left(\frac{nq_0}{N}\right)^2\right]\right\}, \tag{B9}$$

where

$$A_{nq_0} = \frac{6}{n^2(n^2-1)\omega_{q_0}} \sum_{\substack{n_{1,2}=1 \\ n_1+n_2=n}}^{n-1} n_1 n_2 A_{n_1q_0}A_{n_2q_0}. \tag{B10}$$

Expressing $A_{n_1q_0}$ and $A_{n_2q_0}$ via Eq. (19b) (valid because $n_{1,2} < n$) and taking into account that

$$\sum_{\substack{n_{1,2}=1 \\ n_1+n_2=n}}^{n-1} n_1 n_2 \equiv \frac{1}{6}n^2(n^2-1),$$

we obtain

$$A_{nq_0} = \frac{A_{q_0}^n}{\omega_{q_0}^{n-1}}. \tag{B11}$$

Equations (B9) and (B11) coincide with Eqs. (19a) and (19b) at $k=n$, thus concluding the induction.

APPENDIX C: QB STABILITY IN THE β-FPU MODEL

Making a replacement (23) in the equations of motion (5) and keeping only linear in ξ_q terms, we obtain an equation describing the dynamics of infinitesimal deviations from the QB orbit,

$$\ddot{\xi}_q + \omega_q^2\xi_q = -3\rho\hat{Q}_{q_0}^2(t)\omega_{q_0}^2 \sum_{r=1}^{N} b_{qr}\xi_r + O(\rho^2, \xi_l), \tag{C1}$$

where $b_{qr} = \omega_q\omega_r C_{q_0,q_0,q,r}$, and $O(\rho^2, \xi_l)$ denotes a linear form of $\{\xi_l\}$ with small coefficients of the order $O(\rho^2)$.

Inserting here $\hat{Q}_{q_0}(t)$ from Eq. (27), we obtain the following Mathieu equation:

$$\ddot{\xi}_q + \omega_q^2\xi_q = -h(1+\cos\Omega t)\sum_{r=1}^{N} b_{qr}\xi_r + O(h^2, \xi_l), \tag{C2}$$

where $h = 3\rho E_{q_0}$, $\Omega = 2\hat{\omega}$.

In the vector-matrix form it can be rewritten as follows:

$$\ddot{\boldsymbol{\xi}} + \boldsymbol{A}\boldsymbol{\xi} + h(1+\cos\Omega t)\boldsymbol{B}\boldsymbol{\xi} = O(h^2\boldsymbol{\xi}), \tag{C3}$$

where $\boldsymbol{\xi} = (\xi_q)$ is a vector, $\boldsymbol{A} = (a_{qr})$ is a diagonal matrix with elements $a_{qr} = \delta_{qr}\omega_q^2$, and $\boldsymbol{B} = (b_{qr})$ is the coupling matrix.

Further, we analyze parametric resonance in Eq. (C3), treating h and Ω as independent parameters, and then recall their dependence.

In the limit $h \to 0$, the equilibrium point $\boldsymbol{\xi} = 0$ is strongly stable for all values of Ω except for a finite number of values Ω_{nkl} which satisfy

$$\omega_k + \omega_l = n\Omega_{nkl}, \tag{C4}$$

where n is a natural number, and the modes k and l belong to the same connected component of the coupling graph whose connectivity is defined by the matrix $\boldsymbol{B}$. Strong stability implies that this point is also stable for all Hamiltonian systems close enough to the considered one.

Each point $(\Omega_{nkl}, 0)$ on the plane of parameters (Ω, h) is associated with a zone of parametric resonance. Restricting ourselves to the case of primary resonance, which necessarily requires $n=1$ in Eq. (C4), we specify the frequency Ω as

$$\Omega = (\omega_k + \omega_l)(1+\delta), \tag{C5}$$

where the detuning parameter δ is assumed to be the order $\delta = O(h)$. We seek for a solution to Eq. (C3) in the form

$$\boldsymbol{\xi} = \sum_{m=-\infty}^{+\infty} \boldsymbol{f}^m e^{(i\tilde{\omega}_1 + z + im\Omega)t} + \text{c.c.}, \tag{C6}$$

where $\tilde{\omega}_1 = \omega_k(1+\delta)$, $\boldsymbol{f}^m = (f_q^m)$ are unknown complex vector amplitudes, and z is a small unknown complex number. We make an assumption $z = O(h)$, which is confirmed further in the course of the calculation.

Inserting Eq. (C6) into Eq. (C3), we obtain a system of algebraic equations for the amplitudes f_q^m,

$$[2iz(\tilde{\omega}_1 + m\Omega) - (\tilde{\omega}_1 + m\Omega)^2 + \omega_q^2] f_q^m + (h\boldsymbol{B}\boldsymbol{f}^m)_q + \left(\frac{h}{2}\boldsymbol{B}(\boldsymbol{f}^{m+1} + \boldsymbol{f}^{m-1})\right)_q = O(h^2|\boldsymbol{\xi}|). \tag{C7}$$

Note that if the coefficient in square brackets in Eq. (C7) is not a small value of the order $O(h)$, then the corresponding amplitude f_q^m is itself a small value of the order $O(h|\boldsymbol{\xi}|)$. Let us find out for which values of the indices m and q the mentioned coefficient is small. As we assume $z = O(h)$, the difference $-(\tilde{\omega}_1 + m\Omega)^2 + \omega_q^2$ needs to be a small value. It will be so if the absolute value $|\tilde{\omega}_1 + m\Omega|$ is close to one of the eigenfrequencies ω_q. According to the definition of $\tilde{\omega}_1$ and the expression for Ω (C5), this implies $|(m+1)\omega_k + m\omega_l| = \omega_q$. Generically, due to the incommensurate eigenfrequencies spectrum, this condition is only fulfilled for $m=0$, $q=k$ or $m=-1$, $q=l$.

It follows that all amplitudes f_q^m except for f_k^0 and f_l^{-1} are small values of the order $O(h|\boldsymbol{\xi}|)$. Then we are able to write down a closed system for f_k^0 and f_l^{-1} accurate to $O(h^2|\boldsymbol{\xi}|)$,

$$[2iz\tilde{\omega}_1 + 2\omega_k^2(h-\delta)] f_k^0 + \frac{h}{2} b_{kl} f_l^{-1} = O(h^2|\boldsymbol{\xi}|), \tag{C8a}$$

$$\frac{h}{2} b_{lk} f_k^0 + [-2iz\tilde{\omega}_2 + 2\omega_l^2(h-\delta)] f_l^{-1} = O(h^2|\boldsymbol{\xi}|), \tag{C8b}$$

where $\tilde{\omega}_2 = \Omega - \tilde{\omega}_1 = \omega_l(1+\delta)$. Note that for a primary resonance, the coupling coefficient b_{kl} must be nonzero, which means that the mode oscillators k and l are directly coupled.

A nontrivial solution to this system exists if the determinant of the left-hand part [with an error $O(h^2)$ allowed for in each element] equals zero. From this condition, we derive

$$z_{1,2} = -i\frac{(h-\delta)(\omega_l - \omega_k)}{2} \pm \frac{1}{2}\sqrt{\frac{h^2}{4}\omega_k\omega_l - (h-\delta)^2(\omega_k + \omega_l)^2 + O(h^3)} + O(h^2). \tag{C9}$$

In the initial problem, both h and Ω depend on the nonlinearity magnitude βE_{q_0}. This dependence defines a line starting from the point $(2\omega_{m_0}, 0)$ on the (Ω, h) plane. The intersections of this line with the resonance zones are the regions of the QB orbit instability.

The nearest primary resonance corresponds to $k = m_0 - 1$, $l = m_0 + 1$, $n = 1$. In this case, we can derive a simpler expression for $z_{1,2}$ in the vicinity of the bifurcation point (near the edge of the resonance zone) if we let $N \to \infty$ at the same time assuming $q_0/(N+1) = \text{const}$, which means $\omega_{q_0} = \text{const}$.

From Eq. (B4), we obtain

$$\omega_{q_0+1} - \omega_{q_0-1} = 2\cos q_0 \varkappa [1 + O(\varkappa^2)], \tag{C10a}$$

$$\omega_{q_0+1}\omega_{q_0-1} = \omega_{q_0}^2 [1 + O(\varkappa^2)], \tag{C10b}$$

$$\omega_{q_0+1} + \omega_{q_0-1} = 2\omega_{q_0}[1 + O(\varkappa^2)]. \tag{C10c}$$

Then we express δ from Eq. (C5),

$$\delta = \frac{\Omega}{\omega_{q_0+1} + \omega_{q_0-1}} - 1 = \frac{3}{4}h + \frac{1}{2}\varkappa^2 + O(\varkappa^4). \tag{C11}$$

Inserting Eqs. (C10a)–(C10c) and (C11) into Eq. (C9) and taking into account that if we are close to the bifurcation point [the expression under the square root in Eq. (C9) is close to zero] then $h = O(\varkappa^2)$, we find

$$z_{1,2} = \pm\frac{1}{2}\omega_{q_0}\varkappa^2\sqrt{R - 1 + O(\varkappa^2)} + iO(\varkappa^3), \tag{C12}$$

where $R = h/\varkappa^2 = 6\beta E_{q_0}(N+1)/\pi^2$.

According to Eq. (C6), the absolute values of the Floquet multipliers involved in the resonance are calculated as

$$|\lambda_{j_1 j_2}| = \exp\left(\frac{2\pi \mathrm{Re} z_{1,2}}{\Omega}\right), \tag{C13}$$

which finally leads to Eq. (30).

[1] E. Fermi, J. Pasta, and S. Ulam, Los Alamos Report LA-1940 (1955); also in *Collected Papers of Enrico Fermi*, edited by E. Segre (University of Chicago Press, Chicago, 1965), Vol. II, p. 978; *Many-Body Problems*, edited by D. C. Mattis (World Scientific, Singapore, 1993).

[2] J. Ford, Phys. Rep. **213**, 271 (1992).

[3] Focus issue, *The Fermi-Pasta-Ulam Problem—The First Fifty Years*, edited by D. K. Campbell, P. Rosenau, and G. M. Zaslavsky, Chaos 15, No. 1 (2005).

[4] G. P. Berman and F. M. Izrailev, Chaos **15**, 015104 (2005).

[5] N. J. Zabusky and M. D. Kruskal, Phys. Rev. Lett. **15**, 240 (1965).

[6] F. M. Izrailev and B. V. Chirikov, *Statistical Properties of a Nonlinear String* (Institute of Nuclear Physics, Novosibirsk, USSR, 1965) (in Russian); Dokl. Akad. Nauk SSSR **166**, 57 (1966) [Sov. Phys. Dokl. **11**, 30 (1966)].

[7] B. V. Chirikov, Atomnaya Energia **6**, 630 (1959) [J. Nucl. Energy, Part C **1**, 253 (1960)].

[8] J. De Luca, A. J. Lichtenberg, and M. A. Lieberman, Chaos **5**, 283 (1995).

[9] D. L. Shepelyansky, Nonlinearity **10**, 1331 (1997).
[10] P. Bocchierri, A. Scotti, B. Bearzi, and A. Loigner, Phys. Rev. A **2**, 2013 (1970); L. Galgani and A. Scotti, Phys. Rev. Lett. **28**, 1173 (1972); A. Patrascioiu, *ibid.* **50**, 1879 (1983).
[11] H. Kantz, Physica D **39**, 322 (1989); H. Kantz, R. Livi, and S. Ruffo, J. Stat. Phys. **76**, 627 (1994).
[12] L. Casetti, M. Cerruti-Sola, M. Pettini, and E. G. D. Cohen, Phys. Rev. E **55**, 6566 (1997).
[13] F. Fucito, F. Marchesoni, E. Marinari, G. Parisi, L. Peliti, S. Ruffo, and A. Vulpiani, J. Phys. (Paris) **43**, 707 (1982); R. Livi, M. Pettini, S. Ruffo, M. Sparpaglione, and A. Vulpiani, Phys. Rev. A **28**, 3544 (1983).
[14] S. Flach, M. V. Ivanchenko, and O. I. Kanakov, Phys. Rev. Lett. **95**, 064102 (2005).
[15] P. C. Hemmer, L. C. Maximon, and H. Wergerland, Phys. Rev. **111**, 689 (1958).
[16] S. Flach and C. R. Willis, Phys. Rep. **295**, 181 (1998), and references therein.
[17] A. J. Sievers and J. B. Page, in *Dynamical Properties of Solids VII: Phonon Physics, the Cutting Edge* (Elsevier, Amsterdam, 1995); S. Aubry, Physica D **103**, 201 (1997); *Energy Localisation and Transfer*, edited by T. Dauxois, A. Litvak-Hinenzon, R. MacKay, and A. Spanoudaki (World Scientific, Singapore, 2004); D. K. Campbell, S. Flach, and Yu. S. Kivshar, Phys. Today **57**(1), 43 (2004).
[18] S. Flach and A. Gorbach, Chaos **15**, 015112 (2005).
[19] R. S. MacKay and S. Aubry, Nonlinearity **7**, 1623 (1994).
[20] R. Livi, M. Spicci, and R. S. MacKay, Nonlinearity **10**, 1421 (1997).
[21] S. Aubry, Ann. Inst. Henri Poincare, Sect. A **68**, 381 (1998); S. Aubry, G. Kopidakis, and V. Kadelburg, Discrete Contin. Dyn. Syst., Ser. B **1**, 271 (2001).
[22] G. James, C. R. Acad. Sci., Ser. I: Math. **332**, 581 (2001).
[23] S. Flach, Phys. Rev. E **50**, 3134 (1994); J. L. Marin and S. Aubry, Nonlinearity **9**, 1501 (1996); B. Dey, M. Eleftheriou, S. Flach, and G. Tsironis, Phys. Rev. E **65**, 017601 (2001); P. Rosenau and S. Schochet, Phys. Rev. Lett. **94**, 045503 (2005).
[24] S. Flach, Phys. Rev. E **58**, R4116 (1998).
[25] J. H. Conway and A. J. Jones, Acta Arith. **XXX**, 229 (1976); R. Dvornicich and U. Zannier, Monatsh. Math. **12**, 97 (2000).
[26] M. A. Lyapunov, *The General Problem of the Stability of Motion* (Taylor & Francis, London, 1992), pp. 166–180.
[27] A. Zygmund, *Trigonometric Series* (Cambridge University Press, Cambridge, England, 1968).
[28] Note that we do not demand specific symmetries leading to low-dimensional invariant manifolds in phase space, in contrast to the discussion in Refs.[31,38]. Consequently, our QB solutions do not have to be embedded in such subspaces.
[29] The scheme of the instability threshold calculation for the β-model described in Sec. V C fails in the α-model, because the linearized system corresponding to a QB orbit escapes the first-order parametric resonance due to next-order corrections to the shape of the resonance zone, as numerical calculations show.
[30] L. Berchialla, A. Giorgilli, and S. Paleari, Phys. Lett. A **321**, 167 (2004).
[31] R. L. Bivins, N. Metropolis, and J. R. Pasta, J. Comput. Phys. **12**, 65 (1973); B. Rink, Physica D **175**, 31 (2003), and references therein.
[32] J. DeLuca, A. J. Lichtenberg, and S. Ruffo, Phys. Rev. E **51**, 2877 (1995).
[33] The subsequent bifurcations of the same type are associated with next primary resonances of the type $k=q_0-m$, $l=q_0+m$, $n=1$, $m=2,3,\ldots$. The corresponding bifurcation points are located at $R=m^2+O(1/N^2)$. Note that higher-order resonances at certain values of q_0 and N may result in the appearance of narrow instability regions within the region $0<R<1$.
[34] C. F. Driscoll and T. M. O'Neil, Phys. Rev. Lett. **37**, 69 (1976).
[35] J. DeLuca, A. J. Lichtenberg, and S. Ruffo, Phys. Rev. E **60**, 3781 (1999).
[36] A. Giorgilli, S. Paleari, and T. Penati, Discrete Contin. Dyn. Syst., Ser. B **5**, 1 (2005).
[37] I. Daumont, T. Dauxois, and M. Peyrard, Nonlinearity **10**, 617 (1997); M. Peyrard, Physica D **119**, 184 (1998); T. Cretegny, T. Dauxois, S. Ruffo, and A. Torcini, *ibid.* **121**, 109 (1998); M. Johansson, A. M. Morgante, S. Aubry, and G. Kopidakis, Eur. Phys. J. B **29**, 279 (2002); B. Rumpf and A. C. Newell, Phys. Rev. Lett. **87**, 054102 (2001); B. Rumpf and A. C. Newell, Physica D **184**, 162 (2003); G. P. Tsironis and S. Aubry, Phys. Rev. Lett. **77**, 5225 (1996); A. Bikaki, N. K. Voulgarakis, S. Aubry, and G. P. Tsironis, Phys. Rev. E **59**, 1234 (1999); R. Reigada, A. Sarmiento, and K. Lindenberg, *ibid.* **64**, 066608 (2001); S. Flach and G. Mutschke, *ibid.* **49**, 5018 (1994); M. Eleftheriou, S. Flach, and G. P. Tsironis, Physica D **186**, 20 (2003); M. V. Ivanchenko, O. I. Kanakov, V. D. Shalfeev, and S. Flach, *ibid.* **198**, 120 (2004); M. Eleftheriou and S. Flach, *ibid.* **202**, 142 (2005).
[38] N. Budinsky and T. Bountis, Physica D **8**, 445 (1983); Y. A. Kosevich, Phys. Rev. Lett. **71**, 2058 (1993); S. Flach, Physica D **91**, 223 (1996); P. Poggi and S. Ruffo, *ibid.* **103**, 251 (1997).
[39] J. H. Hubbard and B. H. West, *Differential Equations: A Dynamical Systems Approach* (Springer Verlag, Berlin, 1995), pp. 224–229.